ISSN 1063-7710, Acoustical Physics, 2010, Vol. 56, No. 6, pp. 811–830. © Pleiades Publishing, Ltd., 2010.

Nonlinear Theory of Waves in Solid State with Cardinally Changing Crystalline Structure

E. L. Aero and A. N. Bulygin

Institute of Engineering Problems, Russian Academy of Sciences, Bol'shoi prospekt 61, St. Petersburg, 199178 Russia
e-mail: 16aero@mail.ru

Received March 19, 2010

Abstract—A nonlinear theory of propagating periodic and nonlinear solitary waves (like kinks and solitons) related to the motion of defects in crystals and of specific periodic waves into which the former ones transform in the field of the compression stress was developed. The role of intense tension stress leading to the heavy structural rearrangement of the crystal as a result of the effect of the external stress on the interatomic potential barriers was taken into account as well. Crystals with a complex lattice consisting of two sublattices were considered. Arbitrarily large displacements of sublattices were analyzed. The nonlinear theory is based on an additional element of the translational symmetry typical for complex lattices but not introduced earlier in solid-state physics. The variational equations of macroscopic and microscopic displacements turn out to be a nonlinear generalization of the linear equations of acoustic and optical modes obtained by Carman, Born, and Huang Kun. The microscopic displacement fields are described by the nonlinear sine-Gordon equation. In the one-dimensional case, exact solutions of the nonlinear equations were found and their features were revealed. In the case of two-dimensional (2+1) fields, new methods of the exact solutions of the sine-Gordon equation were developed. They describe the interaction of the nonlinear waves with the structural inhomogeneities of solid state due to the external fields of stress and deformations.

DOI: 10.1134/S1063771010060059

1. GENERAL EQUATION

The dynamic theory of the crystalline lattice is well developed at the level of the linear theory [1–3]. However, its generalizations do not reach the limits of anharmonic approximations. A drawback of these classical approaches is that small displacements are considered that do not move atoms out of the cell boundaries. This restriction does not allow one to describe cardinal qualitative changes of its characteristics.

At present this approach is not completely adequate to the new problems arising in the problems of the formation and control of the structure of new materials. Small changes of the internal structure which are predicted by the linear theory, eventually, simply elaborate the changes of the macroscopic geometries of the lattice and lead only to the renormalization of the material constants. The solution of these problems requires the introduction of essentially nonlinear models and a direct account of the deep changes of the structure of the solid state.

The universal approach starting from the remarkable works of the French scientists E. and F. Cosserat [4] is based on the introduction of internal rotational degrees of freedom in the continuum model of the solid state. The multiple attempts of its implementation have shown that, in the linear theory, new effects are indeed predicted. The main new results are the appearance of new modes of the optical oscillations, spatial–temporal dispersion of the elastic properties, and near-boundary effects in statics [5–8].

Transition to the essentially nonlinear equations, as shown in [9–12], enables one to predict deep structural rearrangements, lowering of the potential barriers, switching of the interatomic bonds, the appearance of singular defects and other damage, and phase transformations. But the phenomenological theory has limitations. Of course, one can introduce internal parameters of the microdeformations type into the theory, describing the change of the structure, and even calculate them. However, their physical sense can be revealed if the initial structural state of the body is given and the material scales of the length and time are introduced. This is not done in the continuum theory.

It appears that joint solution of the problem discontinuity and nonlinearity of the models allows one to formulate the new principle of the translational invariance of the energy. E. and F. Cosserat for the first time in mechanics introduced an analogous principle for medium with rotational degrees of freedom. In this work the theory of the nonlinear waves in solid state experiencing the cardinal rearrangement of the crystalline structure is developed.

The proposed theory is based on a model of the complex lattice consisting of two sublattices that are superposed (merge into one) by a shift on a constant

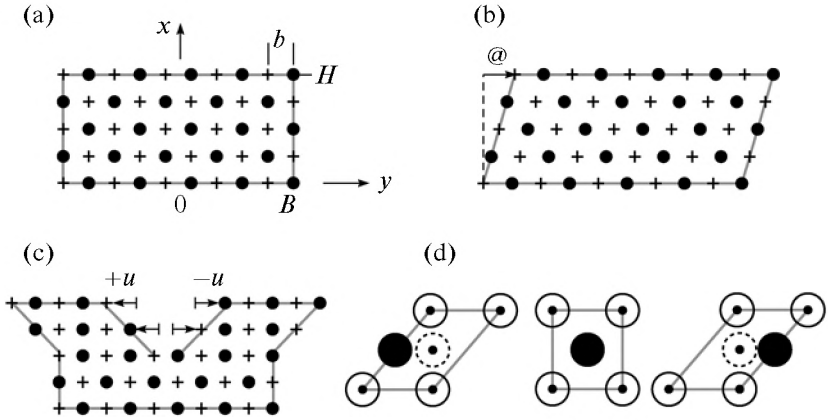

Fig. 1. Complex lattice consisting of two sublattices (a), macroscopic deformation without the shift of sublattices (b), microdeformations at twinning separation (c), and bifurcation of the structure of the unit cell at microdeformation (d).

structural vector $\mathbf{u}_0$, being a parameter of the complex lattice (Fig. 1a).

This model is well known in solid-state physics; however, it is elaborated in the linear and anharmonic approaches. In the linear local theory of the crystalline lattice of Carman, M. Born, and Huang Kun [1], two equations are obtained: for the acoustic **U** and "optical" **u** displacements, respectively. In the work of A.M. Kosevich [2], physical mechanics of the nonideal crystalline lattice accounting for defects was built. I.A. Kunin developed the linear nonlocal theory of the complex crystalline lattice in which the long range is elaborated [3].

In the local nonlinear theory proposed here the main attention is paid to the short-range effect responsible for the cardinal structural change (including the appearance of defects and new phase) and to the so-called reconstruction transitions—changes of the symmetry class of the lattice. The transition to essentially nonlinear equations enables one to predict lowering of the potential barriers and switching of the interatomic bonds.

The introduction of the changes in the local topology by means of the internal degrees of freedom (fields **u**) to the theory turns out to be effective if the generalization of the linear approach is performed as follows. Consider the arbitrarily large displacements of sublattices **u**. The additional element of the translational symmetry typical for the complex lattices, but not introduced in solid-state physics earlier, is the basis of building the nonlinear theory. Obviously, displacement of one sublattice with respect to the other for one period (or their integer number) up to superposing the sublattice with itself once again reproduces the structure of the complex lattice. Thus, the energy of the complex lattice should be a periodic function of the relative rigid displacement of sublattices **u** invariant to such translation. Of course, the classical principle of the translational symmetry leading to the invariance of the lattice energy to the joint translation **U** of both sublattices by one period of the complex lattice remains. Such an approach allows one to introduce new crystal parameters in micromechanics, on the basis of which it is possible to describe micromechanisms of the cardinal structural rearrangements of the lattice. These are short-range characteristics, potential barriers, typical sizes of the structure elements and interphase boundaries, and bifurcation parameters.

The displacements of the center of the inertia of pairs of atoms (unit cell) and their relative displacement inside the cell (due to the change of $\mathbf{u}_0$) are introduced as follows:

$$\mathbf{U} = (m_1\mathbf{U}_1 + m_2\mathbf{U}_2)/(m_1 + m_2),$$
$$\mathbf{u} = (\mathbf{U}_1 - \mathbf{U}_2)/b. \qquad (1)$$

Here, $\mathbf{U}_1$ and $\mathbf{U}_2$ are the displacements of atoms (with masses m_1, m_2) of the first and the second sublattices, respectively, and b is the period of sublattices.

A very simple one-dimensional and one-component case is considered which can be analyzed exactly and to the end in the general form. The conditions of the one-dimensional and one-component motion are as follows:

$$U_i \to U(t,x), \quad u_i \to u(t,x).$$

In this section U and u are any vector component, but not the absolute value of the vector. The variational equations of the motion determining the $U(t,x)$, $u(t,x)$ fields are built. The Lagrangian

$$L = (1/2H)\int_0^H [\rho \dot{U}_n \dot{U}_n + \mu \dot{u}_n \dot{u}_n - 2d]dx$$

is the starting point. Here, ρ is the average density of the atomic mass, μ is the so-called density of the reduced masses of pairs of atoms (these values differ in the case of atoms with different masses), d is the energy of macro- and microdeformations, H is the size

of the region, and the thickness of the plane-parallel layer of the crystal. The dots on top mark time derivatives.

The invariant expression with account of the interaction (nonlinear mechanical striction—rearrangement microstructure under the action of macroscopic deformations, hereinafter, simply, striction) of the $U(t, x)$, $u(t, x)$ fields is

$$d = [(\lambda/2)(U_{,x})^2 + (k/2)(u_{,x})^2 + (p - sU_{,x})(1 - \cos u)], \quad (2)$$

where $U_{,x}$ and $u_{,x}$ are the macro- and microscopic gradients; λ, k are macro- and microscopic modules; s is the coefficient of nonlinear striction; $2p$ is the interatomic potential barrier in the nondistorted lattice (the activation energy of the atomic bonds in the unit cell); and the comma in the tensor indices marks spatial derivatives. The gradient terms in expression (2) provide its invariance at macrotranslations, and the periodic term $\cos u$ provides invariance of the energy to the mutual translations of the sublattices in a certain and fixed direction. In the one-dimensional theory, the changes of the value of the microdisplacement vector, but not of its direction, are taken into account. More general cases are considered in [6–8].

By varying the functional $\int L dt$ on displacements u; gradients $U_{,x}$, $u_{,x}$; and velocity $\dot{U}$, $\dot{u}$ and equating its variation with zero, the system of two connected equations of the Euler–Lagrange type for two fields—acoustic macrodisplacements and optical microdisplacements—is obtained:

$$\rho \ddot{U} = \lambda U_{,xx} - [s(1 - \cos u)]_{,x}, \quad (3)$$

$$\mu \ddot{u} = k u_{,xx} - (p - sU_{,x}) \sin u. \quad (4)$$

The first equation (acoustic oscillations) takes into account both the long-range forces depending on the gradients of macrodisplacements (deformations) $U_{,x}$ and the forces due to the structural changes depending on the gradients of microdisplacements $u_{,x}$. The second equation ("optical" oscillations) contains the nonlinear forces of the interaction of sublattices (the second term on the right), which have a periodic character due to the invariance of the complex lattice with respect to the shifts of sublattices by one period. Note that microdisplacements are measured in the units of the lattice period.

The problem of the initial and boundary conditions for system (3) and (4) is discussed with reference to the partial problems of the propagation of the localized waves. These equations in the linearized form not taking into account the effect of mechanical striction are obtained for the first time in the dynamic theory of the crystalline lattices [1] and are known in the literature as equations of acoustic and optical oscillations of the complex lattice. Weak nonlinearity at the level of anharmonicities of different degrees has been used in lattice mechanics long ago. However, strong nonlinearity allowing the transitions of atoms to the neighboring cells (reconstruction transitions), for the first time was introduced in our works [7–9]. In addition, we used nonlinear striction forces (last terms on the right), implementing the micromechanism of the cardinal rearrangement of the structure in Eqs. (3) and (4). If these terms are ignored, the equation of the classical theory of elasticity and the independent equation of the microshift of sublattices are obtained in the limit.

Turning to dynamics, the consideration is limited to the processes of the propagation of the nonequilibrium perturbations with the constant velocities (problem "without initial conditions") when both fields are a function of the wave phase q,

$$q = x - Vt, \quad (V > 0, V < 0). \quad (5)$$

Here, V is the constant phase velocity (two signs of the velocity refer to two waves propagating in opposite directions). It is difficult to set the arbitrary initial states. In this case the stationary modes necessary for the existence of the solitary waves require searching for quite complicated solutions of Eqs. (3) and (4).

By limiting ourselves to (5) in Eqs. (3) and (4), two conventional differential equations,

$$\lambda(1 - V^2/V_s^2) U_{,qq} = [s(1 - \cos u)]_{,q}, \quad V_s^2 = \lambda/\rho, \quad V_k^2 = k/\mu, \quad U_{,q} \to \partial U/\partial q, \quad (6)$$

$$k(1 - V^2/V_k^2) u_{,qq} = (p - sU_{,q}) \sin u, \quad u_{,q} \to \partial u/\partial q, \quad (7)$$

are obtained, where V_s and V_k are phase velocities of the acoustic and optical modes, respectively:

$$V_s^2 = \lambda/\rho, \quad V_k^2 = k/\mu. \quad (8)$$

By integrating (3), it can be written

$$\lambda(1 - V^2/V_s^2) U_{,q} = s(1 - \cos u) + \sigma. \quad (9)$$

The integration constant σ is the external constant field of stress. With its help macrogradients are excluded from Eq. (7). The separate equation for the optical mode is obtained:

$$l_0^2 p(1 - V^2/V_k^2) u_{,qq} = \tilde{p}_1 \sin u + \tilde{p}_2 \sin u \cos u. \quad (10)$$

Here the following notation is used:

$$\tilde{p}_1 = p - s\frac{s + \sigma}{\lambda(1 - V^2/V_s^2)}, \quad (11)$$

$$\tilde{p}_2 = \frac{s^2}{\lambda(1 - V^2/V_s^2)}. \quad (12)$$

Nonlinear equation (10) is a generalization of the known sine-Gordon equation, the solution of which, at definite boundary conditions, is solitary and peri-

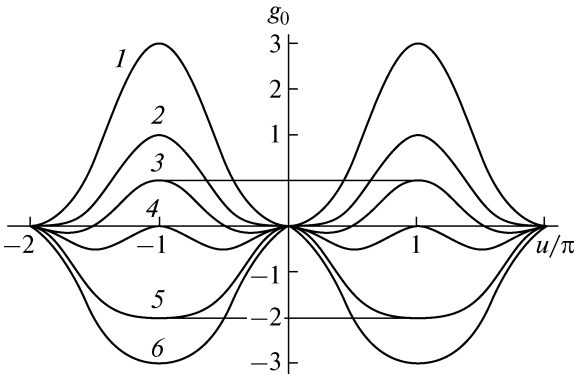

Fig. 2. Potential energy of microoscillations at different stress (curve *1* corresponds to the tension stress, curve *6* to the compression stress).

odic waves. As a result of its single integration, the expression for the square microgradient is obtained:

$$(\tilde{l}_0^2/2)p(u_{,q})^2 = \tilde{P}(1-\cos u) - (\tilde{p}_2/2)(1-\cos u)^2 + G. \quad (13)$$

Hereinafter,

$$\tilde{l}_0^2 = l_0^2(1 - V^2/V_k^2), \quad l_0^2 = k/p, \quad (14)$$

$$\tilde{P} = p - \frac{s\sigma}{\lambda(1 - V^2/V_s^2)}. \quad (15)$$

The first relation introduces the characteristic length l_0 and the characteristic time $l_0 V_k = k/\sqrt{p\mu}$, which is a discriminating feature of this theory.

In Eq. (13), a new integration constant G appears alongside with σ, which was already introduced. Obviously, both constants are connected with the boundary conditions superimposed on the values of the function itself and its gradient $u_{,q}$. The physical meaning of the constant G can be clarified by considering the situation at the boundary $x = 0$, when $q = q_0 = -Vt$. Then $u_{,q} = u_{,t}$ is the velocity of the oscillations of the model pendulum, and the left-hand part of relation (13) is its kinetic energy. The right-hand part depending on u can be formally considered as the potential energy $g_0(u)$ (with the minus sign):

$$(\tilde{l}_0^2/2)p(u_{,q})^2 + g_0 = G; \quad g_0 = -\tilde{P}(1-\cos u) + (\tilde{p}_2/2)(1-\cos u)^2. \quad (16)$$

Here, the first relation expresses the law of conservation of energy.

Figure 2 shows the $g_0(u)$ function as a series of curves at different values of the parameter $\tilde{P}$ linearly dependent on the stress σ. The presence of diversely alternating maxima and minima determines several different modes of the nonlinear oscillations of the lattice microstructure or several wave branches.

In the considered approach the constant G plays the role of the permanent total energy of the microstructure oscillations and is presented by the first relation in (16). The value of this energy affects the picture of the wave branches, but it is only a part of the total energy of the oscillations of the whole system with macroscopic and microscopic degrees of freedom. In the one-dimensional case, the stress σ is a constant, and in such a case, the region of microoscillations determined by the two integration constants, G and σ, can be considered separately.

The total energy G (Fig. 2) determines three bifurcation levels separating the different modes of the oscillations. The levels are denoted by the horizontal lines one of which is the abscissa axis. The upper level is the horizontal line connecting the maxima of potential curve *3*, which has two shallow minima under the abscissa axis. The wave localized between the corresponding maxima of the microdisplacement values refers to the motion between the points of contact with maxima. There are no minima above this level (at large G values), and the motion mode is reduced simply to oscillations in the periodic potential with the zero minima (curves *1* and *2*), which is characteristic for weakly distorted lattices. On the contrary, with decrease in the energy value to the zero level, another potential relief with the new equilibrium positions is formed. At $G = 0$, the potential (curve *4*) with the two additional minima appears. The lattice changes its microstructure cardinally. With further decrease in the energy G to negative values, the new potential relief degenerates and once again transfers to the relief with the former number of extrema but inversed. The bifurcation point is denoted by a horizontal line connecting minima of curve *5*. It is important that the cardinal rearrangement of the microstructure is connected with the stress value. This is seen from expression for the potential energy (16) containing the coefficient $\tilde{P}$ linearly dependent on stress according to formula (15).

These qualitative features can be revealed for the solution of Eq. (13) if its phase "portrait" is built (see Fig. 3). The "portrait" corresponds to the value $p_1 = 4/3$. The vertical axis shows the value of "velocity" $u_{,q}$ or microgradient $u_{,x}$ if $V = 0$, and the horizontal axis shows microdisplacements u. Each curve corresponds to one solution determined by the integration constant value from the range $G = -0.3, 0, 0.3, 1, 2$. The total ensemble of the solutions is separated into three groups by separatrices denoted by the dashed curves.

"Small" separatrices ($G = 0$) looking like a figure-eight (short dashes 4) limit the region inside which there are the solutions 5 in the form of closed curves with centers corresponding to the states of the stable equilibrium. The periodic dependences $u(x)$ being a subfamily of partial solutions correspond to the closed curves 5. The periodic solutions 3 are given by the

functions $u(x, t)$ oscillating close to zero. The solutions 5 oscillate around a certain average level $u_a \neq 0$. In such a manner, the nonlinear effect of the dynamic "expansion" due to the asymmetry of the potential wells is revealed. Finally, the drifting modes when the oscillating solution contains the linear component $\Delta u = q = x - Vt$ correspond to the solutions 1. These are modulated domain nanostructures. Their explicit form will be presented below. They are limited by both the microdisplacement and microgradient values. It is important that the smallest values of the constant G, i.e., the gradient energy $k(u_{,x})^2$ (at $u = 0$) correspond to them.

The family of the periodic solutions 3, closed curves covering both mentioned equilibrium centers limited by the "large" separatrix 2 ($G = 1$) (denoted by long dashes), lies outside the "small" separatrix (at large energy values). These solutions are related to the large microdisplacements of the neighboring atoms, not leaving, however, the limits of the unit cell.

The region of the open curves *1* corresponding to the solutions not limited by the microdisplacement value is outside the "large" separatrix (at large G). These solutions describe the plastic flow of the lattice.

It is possible to return to the formal analogy with the oscillations of the pendulum system (considering the $u_{,q}$ value as the pendulum velocity) and present the demonstrative picture of its passage through some potential barriers. The equilibrium points of the two potential wells separated by the potential barrier in the self-crossing point of the "small" separatrix correspond to the two mentioned centers. The transition over this barrier with the final velocity (at large G values) corresponds to the closed curves covering the given separatrix. If the transition velocity tends toward zero, the pendulum reaches the bifurcation point (unstable equilibrium)—the saddle point of the self-crossing of the separatrix. Since the time of staying close to the separatrix is large, the corresponding states are of practical interest. These are solitons of the microdisplacement field or lattice defects. Their physical meaning is clarified below.

The unstable state on top of the higher potential barrier corresponding to the second saddle point of self-crossing of the separatrix ($|u| = \pi$, $u_{,x} = 0$) corresponds to the second ("large") separatrix 2. Kink solutions that also describe the structure defects are implemented on the "large" separatrix.

In Fig. 4 different modes of the periodic oscillations are presented by subregions separated by boundaries to which the solitary waves in the form of kinks and solitons correspond. The value of the effective potential barrier $\tilde{P}$ is shown on the abscissa axis. According to definition (11), this is a linear function of stress σ. The plane of the integration constants is divided by the coordinate axes and the direct line $G = -2\tilde{p}_1 = -2(\tilde{P} - \tilde{p}_2)$ into regions of the different solutions of system (6), (7). Numbers 1–6 denote the regions of existence of the periodic solutions. The boundaries between regions form a horizontal line (the ray of the positive abscissa axis) $G \geq 0$ and an inclined line given by the equation $G = -2\tilde{p}_1 = -2(\tilde{P} - \tilde{p}_2)$. The periodic solutions of the regions 4 and 5 are given by functions $u(x, t)$ oscillating close to zero. The solutions 3 and 2 oscillate around a certain average level $u_a \neq 0$. This is the manifestation of the nonlinear effect of dynamic "expansion" due to the asymmetry of the potential wells. Finally, the drifting modes when the oscillating solution contains the linear component correspond to the region 1.The objects of this study are special solutions corresponding to the points of the inclined and horizontal boundaries mentioned above. The points of the boundaries belonging to the regions marked in Fig. 3 with bold lines correspond to the localized solutions of the kink type (dislocations) and

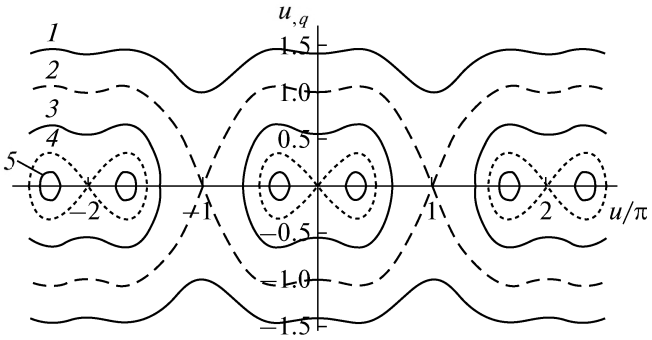

Fig. 3. Phase portrait of microoscillations.

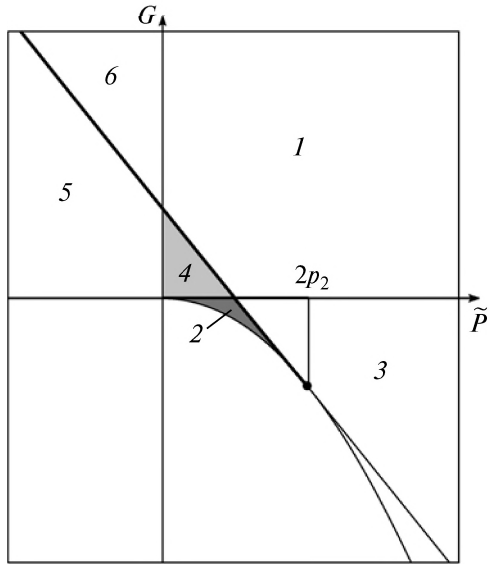

Fig. 4. Map of regions of the different solutions of microwave equation (13) depending on the integration constants G and $\tilde{P}(\sigma)$.

solitons (defects of packing). The points on the continuations of the bold lines to the right marked with thin lines correspond to the special periodic solutions to which the solitary solutions transform. These (solitary and periodic) solutions are considered in the following sections. The solutions not related with kinks and solitons belonging to regions 1–6 are not considered here.

2. STRUCTURAL TRANSITION IN STATICS

In the beginning, some problems of the rearrangement of the lattice in the field of the external stress regardless of the explicit type of the solution of equation (10), i.e., regardless of the boundary conditions are considered. This equation contains the structurally sensitive parameter $\tilde{p}_1$, the coefficient in front of the first term on the right, and the effective interatomic barrier dependent on the external stress. It can be zero and even change its sign to which the bifurcation point of the solution of Eq. (10) corresponds. As a result, a new structure of the lattice with new properties appears.

The case of the static structures is considered. By assuming in formulas (11) and (12) that the velocity V is zero and referring to the static notations p_1 and p_2, one can write

$$\tilde{p}_1 \to p_1 = p - \Delta p, \quad \Delta p = s(s+\sigma)/\lambda. \tag{17}$$

Here, p_1 means the static value of the effective interatomic barrier $\tilde{p}_1$, which differs from the potential p of the ideal nondistorted lattice by the value Δp. The latter is called weakening of the lattice in the field of stress.

The total weakening of the lattice is reached in the first bifurcation point when the value of the effective barrier p_1 is zero, when

$$\Delta p = p \text{ or } (s+\sigma) = p\lambda, \tag{18}$$

i.e., the striction effect compensates (smooths) the initial interatomic barrier. Since by definition $p > 0$ and $\lambda > 0$, then $\Delta p > 0$. Note that, otherwise, weakening in the field of stress is impossible. A certain threshold value of stress corresponds to this point of the structural transition. It depends on the sign of the striction coefficient. If $s > 0$, then

$$\sigma = \sigma_{t1}, \quad \sigma_{t1} = p\lambda/s - s. \tag{19}$$

If $s < 0$, then

$$\sigma = \sigma_{t1}, \quad \sigma_{t1} = -(p\lambda/|s|) + |s|. \tag{20}$$

Here, σ_{t1} is the threshold value of stress at which the structure of the lattice rearranges as a result of weakening of the interatomic bonds. Note that the rearranged structure exists at the conditions $\sigma > \sigma_{t1}$ ($s > 0$) and $\sigma < \sigma_{t1}$ ($s < 0$) and the weakened structure exists at the inverse signs of the inequalities.

The case in which the first coefficient of Eq. (13) becomes zero corresponds to the second bifurcation point, i.e., the condition $\tilde{P} = 0$ or $p_1 = -p_2$. In the unfolded form, it takes the form of the criterion for stress:

$$\sigma = \sigma_t, \quad \sigma_t = p\lambda/s.$$

For the positivity of the p and λ values to hold, s and σ have to be of the same sign.

The third special point $p_1 = p_2$ is the boundary of the region of existence of the solutions of the solitary wave type. It is achieved at the following threshold value of stress:

$$\sigma = \sigma_{t2}, \quad \sigma_{t2} = (p\lambda/s) - 2s = \sigma_{t1} - s, \quad s > 0,$$

and the positive value of the potential barrier corresponds to this point. The zero value corresponds to the first point. This is not the only difference. The bifurcation points delimit the different lattice structures. In statics the structural differences are revealed in different dependences of the amplitude on energy, for example, as shown for solitons in [8]. The considered criteria of hardening and weakening are important in the analysis of the mobility of defects at various conditions of stress.

3. CONDITIONS OF THE APPEARANCE OF THE SOLITARY WAVES

The solutions of Eqs. (10) or (13) are presented as noted above by three modes: nonlinear periodic waves proper, kinks, and solitons. Only kinks and solitons are considered in this section. The conditions of their appearance are the boundary conditions as well.

The equation of the moment transfer of pulse (13) has, generally speaking, two soliton branches determined by the condition imposed on the integration constants G and σ in this equation. These boundaries between the regions are $G \geq 0$, the ray of the positive abscissa axis, and $G = -2\tilde{p}_1 = -2(\tilde{P} - \tilde{p}_2)$, the inclined line, shown in Fig. 3. The special case $G = 0$ is not considered. Excited perturbations depending on stress are considered. They correspond to the case of the appearance of the extreme excitations $u = \pi$ (the displacement by half of the period) in infinitely distant points $|q| \to \infty$, where the gradients of this field on coordinates and time become zero. In fact, from expression (13) for the first integral, one can see that at the values $u = \pi$, $u_{,q} = 0$ the notation for the constant G takes the type:

$$G = -2\tilde{p}_1 = -2(\tilde{P} - \tilde{p}_2). \tag{21}$$

Here, $\tilde{p}_1$ is the dynamic quantity determined by (11). For the solitary waves of the kink and soliton type to appear, this relation, taking into account the specified boundary conditions, should hold. The second con-

stant σ is in the right-hand part according to expressions (11) and (12) and allows one to meet one more boundary condition, finally determining the kink or soliton solution. In other word, for kinks it is necessary to take into account as well the condition in the center ($q = 0$), namely, $u = 0$. By means of expressions (13), (11), and (21), the relation

$$\tilde{l}_0^2(u_{,q})_0^2 = -2p + 2s\frac{s+\sigma}{\lambda(1-V^2/V_s^2)}, \quad (22)$$

which links the slope in the inflection of the kink with the integration constant σ, was obtained.

A similar relation for the soliton is obtained from the condition $u = u_e$, where u_e is the extreme value in its center (amplitude). It should be taken into account that, in the soliton center, $u_{,q} = 0$, i.e., the microgradient becomes zero. Taking this condition into account, from (13), the relation

$$0 = \tilde{P}(1-\cos u_e) - (\tilde{p}_2/2)(1-\cos u_e)^2 - 2\tilde{p}_1 \quad (23)$$

is obtained. According to (11) and (12), it links the soliton amplitude with stress σ contained in coefficients $\tilde{p}_1$ and $\tilde{P}$. This relation allows, generally speaking, the transition (for solitons) to a new integration constant, amplitude u_e.

Note that the general relation (21) (for kinks and solitons) alongside with the specified two constants contains the wave velocity as well (see expressions (11) and (12)). Since these constants are determined by the boundary conditions, equality (21) can be considered as the definition of the velocity of the propagation of a kink or soliton. In the unfolded form, this condition is written as follows:

$$\tilde{p}_1 = p - (1-V^2/V_s^2)\Delta p.$$

Here, Δp is determined by expression (17). Thus, the dependence of the propagation velocity on stress and the potential barrier value is as follows:

$$V^2/V_s^2 = 1 - s\frac{s+\sigma}{\lambda(p-\tilde{p}_1)}. \quad (24)$$

The constant on the right to σ can be expressed in terms of the soliton amplitude and the kink slope in the center by means of formulas (22) and (23).

It should be noted that, in statics ($V = 0$), the corresponding values σ and p_1 are related as

$$\tilde{p}_1 = p_1, \quad p_1 = p - s(s+\sigma)/\lambda. \quad (25)$$

In other words, in the case of standing defects, their characteristics such as the amplitude, slope in the center and, as seen below, width are connected between each other.

In dynamics, according to (24), the energy is spent on the motion of defects as well. Therefore, (25) can be considered as the condition of the threshold excitation (for example, by means of laser irradiation) of the flow of the mechanical perturbations—solitary waves inside the sample. If the external loads (stress) are absent, $\sigma = 0$, then from (24) the expression for V_{ss}, the propagation velocity of the corresponding free oscillations follows:

$$V_{ss}^2/V_s^2 = 1 - s^2/\lambda(p-\tilde{p}_1), \quad V_s^2 = \lambda/\rho. \quad (26)$$

It is important that this characteristic is determined only by the properties of the crystal and is the propagation velocity of the nonlinear sound wave, taking into account the structural softness of the crystal. It is less than the velocity of the linear sound wave.

Then it is possible to introduce the effective dynamic module of elasticity $\tilde{\lambda}$ analogous to the determination of the velocity of the linear sound wave (8):

$$V_{ss}^2 = \tilde{\lambda}/\rho. \quad (27)$$

Then from (26) it follows:

$$\tilde{\lambda} = \lambda - s^2/(p-\tilde{p}_1).$$

This relation means that the crystal with rearranged structure is softer and the typical velocity V_{ss} is less than the linear sound velocity V_s.

One should not think that, in general, only subsonic waves propagate in the crystal. Only free vibrations were mentioned. Upon the effect of the external loads, supersonic waves are possible as well. In the general case, when stress σ differs from zero, the velocity V according to (24) depends on stress as well. By using definition (27), (24) can be rewritten as a dependence of the effective coefficient of dynamic elasticity on stress as well:

$$\tilde{\lambda} = \lambda\left(1 - \frac{\Delta p}{p-\tilde{p}_1}\right) = \lambda - s\frac{s+\sigma}{(p-\tilde{p}_1)}.$$

Now the effective module of dynamic elasticity is not necessarily less than the real one. Everything depends on the sign of the second term on the right in this expression. Depending on the value and sign of stress both weakening, $\Delta p > 0$, and hardening, $\Delta p < 0$, of the crystal can take place. These cases are characterized above.

The external impact leads to decrease in the elastic properties when $\Delta p > 0$ and criteria for stress (18), (19), and (20) hold. In this case formula (24) gives the dependence of the propagation velocity on stress and material parameter.

4. SOLITARY WAVES

Now one of the localized solutions of Eq. (13) satisfying condition (21) is considered. The solution is

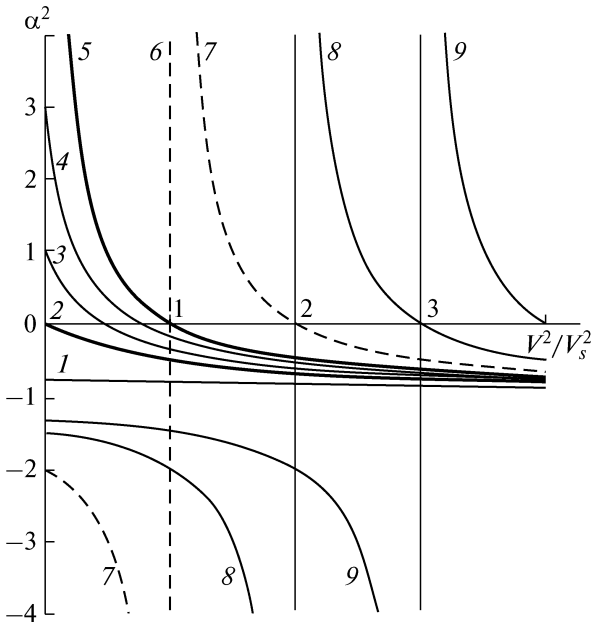

Fig. 5. Dependence of the amplitude multiplier α on the wave velocity at different values of the parameter $S(\sigma)$.

excited in the range of the relatively weak impacts at $\tilde{p}_2 > \tilde{p}_1 > 0$ and has the form

$$u = \pm 2\arctan(\alpha\cosh\zeta),$$
$$\zeta = (q - q_0)/L = (b - x + Vt)/L. \tag{28}$$

Here the double signs on the right correspond to the pair of the possible solutions. In addition, the notation

$$\frac{l_0^2}{L^2} = \frac{\tilde{p}_2 - \tilde{p}_1}{1 - V^2/V_k^2}, \quad l_0^2 = k/p, \tag{29}$$

$$\alpha^2 = \frac{\tilde{p}_1}{\tilde{p}_2 - \tilde{p}_1} = \frac{1 - V^2/V_k^2 - S + s^2/\lambda p}{S - 1 + V^2/V_k^2},$$
$$S = s\frac{2s + s\sigma}{\lambda p} \tag{30}$$

is used. In statics similar solutions are considered in [7].

Solution (28) is a soliton (on a pedestal π) with the center $q = q_0$ and width L or a defect of packing in a crystal of the type of the accumulation of vacancies. The soliton is changed with approaching the boundary of solution (28) or the bifurcation point $\tilde{p}_1 = 0$. Its width (depending on the velocity as well) decreases; the amplitude (the displacement from the pedestal level downward) increases, tending to the limiting value ($\to \pi$); and the amplitude multiplier $\alpha \to 0$. The velocity increases approaching the threshold value V_1, which at the basement (24) satisfies the expression

$$V_1^2/V_s^2 = 1 - s\frac{s + \sigma_0}{\lambda p}.$$

The further narrowing of the width and increase in the velocity do not occur since they are associated with the transition of the value in region of imaginary values. On the contrary, it is possible that the velocity decreases to the zero level that corresponds to the stationary defect, and this is observed at stress

$$\sigma_0 = \frac{\lambda p}{s} - s.$$

On the contrary, with approaching the other boundary of the region ($\tilde{p}_1 = \tilde{p}_2$) the amplitude multiplier increases infinitely. The amplitude tends to zero, and in all space the pedestal level $u = \pi$ is reached (defect of the packing is spread). The velocity takes the value V_2:

$$V_2^2/V_s^2 = 1 - S, \quad S = s\frac{2s + \sigma_0}{\lambda p}.$$

Thus, soliton (28) exists only in the interval of the velocities ($V_1 - V_2$). Its value does not depend on stress and is given by expression

$$\frac{V_1^2 - V_2^2}{V_s^2} = \frac{s^2}{\lambda p},$$

and the amplitude of the multiplier α obviously depends in the velocity and stress σ.

Function (30) is shown in Fig. 5 for different values of the parameter S. For formula (28) to determine the real solution, it is necessary that two conditions hold simultaneously: $\alpha^2 > 0$ and $\frac{l_0^2}{L^2} > 0$, which correspond to the upper region of curves lying between two bold curves *2* and *5*. The values of the parameter $S = 1$ and $S = 1.5$ correspond to these regions and, most important, tension (positive) stress. Interestingly, inside this region the velocity dependences for the originally stationary solitons (they start from the ordinate axis) are located.

Note that, generally speaking, the microdisplacement u_0 in the center of soliton (microamplitude) if written as $\alpha = \tan\frac{u_0}{2}$ has a clearer physical meaning than the amplitude multiplier α. The value $\pi - 2\arctan\alpha = \pi - u_0$ is the microdisplacement with respect to the pedestal level. By using relation (30), it is possible to express the microamplitude u_0 in terms of the velocity and parameter S or stress. On the other hand, according to (29), the microamplitude related to them in terms of the width of the defect L in the

center of which the microdisplacement u_0 is implemented.

Having the solution for the microfield, it is possible to transfer to the macroscopic field U. It is useful to rewrite (28) as follows:

$$1 - \cos u = \frac{2\alpha^2 \cosh^2 \zeta}{1 + \alpha^2 \cosh^2 \zeta}.$$

By using the obtained expression in formula (9), the corresponding explicit expression for the macroscopic field of deformations can be found:

$$\lambda(1 - V^2/V_s^2) U_{,q} = s \frac{2\alpha^2 \cosh^2 \zeta}{1 + \alpha^2 \cosh^2 \zeta} + \sigma. \qquad (31)$$

It is clear that these deformations are induced by microscopic defect (28). Note that the even function of the argument in (31) has a bell-like (soliton-like) form.

The other solitary solution corresponding to the branch $G/2 = -\tilde{p}_1$ but in the other range of stress values ($p_1 \le 0$), is given by the formula

$$\begin{gathered} i = \pm 2 \arctan(a \sinh \zeta), \\ a^2 = -\alpha^2 = -\tilde{p}_1/(\tilde{p}_2 - \tilde{p}_1), \quad \zeta = (q - q_0)/L, \end{gathered} \qquad (32)$$

where the double signs on the right correspond to the pair of possible solutions. In addition, L is the typical size of the region of the localization of the solution (kink), which is present in expression (29). However, the amplitude multiplier a defined here is a somewhat different manner than in (30). It is related to the amplitude multiplier α via the imaginary unity. If the amplitude multiplier a and the width L are real quantities, then the microscopic field $u(\zeta)$ is a real quantity too. It is clear that a^2 should be negative. The region below the abscissa axis and below the boundary curve *5* in Fig. 5 corresponds to this multiplier. The latter excludes as well the region of the imaginary values of the width L (curves *7–9*) corresponding to the values of the parameter $S < 1$. Thus, the amplitude multiplier depends not only on the velocity, but also on stress.

Solution (32) describes the kinklike defect (with the center $u = 0$ in the "point" $q = q_0$) and with limits $u \to -\pi, \pi$ (at the infinite distance from the center). In the linear approximation on ζ, the expression for the Peierls dislocation is obtained [2]. The same as in the case of soliton, the microdisplacement u_0 at the phase origin when $q = 0$ has a clearer physical meaning than the amplitude multiplier. At the same time, in the kink center, $q = q_0$. The constant q_0 can be chosen so that at the boundary $q = 0$ the microdisplacement reaches the preassigned value $u = u_0$.

Then from solution (32) the relation

$$\tan^2 \frac{u_0}{2} = a^2 \sinh^2 q_0 \qquad (33)$$

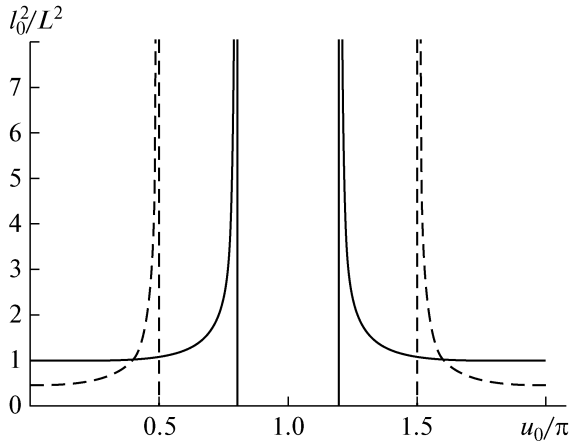

Fig. 6. Dependence of the inverse width of the defect on the microdisplacement on the boundary of the defect layer.

follows. By using (33) and notation (29), (30), the formula

$$\frac{s^2}{\lambda p} \frac{L^2}{l_0^2} = 1 - \frac{\tan^2 u_0/2}{\sinh^2 q_0} \qquad (34)$$

is obtained. The quantity L^2/l_0^2 deduced in this way is useful at the formulation of the problem of the motion of the layer (plane defect) $q_0 = b$ thick containing the considered kink. Formula (34) shows at what values of the microdisplacement u_0 at the boundary of the plane defect $q = 0$ a kink (32) with the relative width (L/l_0) appears inside it. This dependence is shown in Fig. 6 for different values of the parameter $s^2/\lambda p$.

Figure 6 shows that for the existence of the kink a limited value of the microdisplacement $u_0 \le \pi \arctan \sinh b$ is necessary. The equality sign corresponds to the vertical asymptote limiting the region of the solution. The kinks with the width of $L^2/l_0^2 \approx (\lambda p)/s^2$ appear. At large values of the microdisplacement at the boundary layer at $u_0 = \pi \arctan \sinh b$, continuous kinks (32) degenerate into the defects with the zero width ($l_0^2/L^2 \to \infty$), i.e., in the system of the breakups of the microdisplacement field. Due to the ambiguity of the arctangent function $u_0 \to \pi \pm 2n\pi$ at $b \to \infty$. This means that the microdisplacement equal to half of the lattice period is reached (with accuracy to the integer number of periods) only at the boundary infinitely distant from the kink center, whereas in its center it is zero. In a limited-size body containing kinks, the output of dislocations on the surface with the formation of steps is possible.

Interestingly, the restrictions of such kind do not arise in the case of solitons. Similar dependences of the quantity l_0^2/L^2 on the microdisplacement u_0 on the

boundary of the layer (defect) $q = 0$ exist at all u_0 values, and its maximum corresponds to $u_0 = 0; 2\pi$, where defects are the narrowest.

Just as in the case of the soliton, the constant b can be chosen so that, at the boundary of the semispace $x = 0$, the microdisplacements reached the preassigned value $u = u_0$. To this end, kink (32) should meet the condition

$$\frac{l_0^2}{L^2} = \beta_0 \sinh^2 b / \left(\sinh^2 b - \tan^2 \frac{u_0}{2}\right). \quad (35)$$

Unlike the soliton, other dependences on microdisplacements correspond to the kink. Figure 6 shows asymptotes of the infinite l_0^2/L^2 values (zero values of the kink width or thickness of the boundary layer) at the boundary values of the microdisplacements $\left(\tan^2 \frac{u_0}{2} = \sinh^2 b\right)$, which follow from expression (35). It should be emphasized that such values exist always. This intensification of the kink defect (up to a breakup) is due to the velocity dependence of the l_0^2/L^2 value, which is considered below.

Note that the curves in Fig. 5 located in the "corridor" between curves *2* and *5* come from the point of the ordinate axis and cross the abscissa axis. They correspond to the stationary defects, which then begin to move and, at a certain velocity, transform into breakups propagating with supersonic velocities. One of the differences of kinks from solitons is their region of existence on the velocity axis seen in Fig. 5. Thus, solitons are slow defects, the velocity of which is much less than the velocity of the linear sound wave V_s.

On the contrary, the kinks can move with supersonic velocity and also greatly exceed it, reaching the level of the velocities of the optical mode. Curve *1* in Fig. 5 with the amplitude multiplier $a^2 = -\alpha^2 \approx 1$ nearly instantly comes to the region of indefinitely large velocities. The amplitude multiplier in the solution (32) tends to unity. The limiting condition $a = 1$ means an infinitely fast sliding of the kink.

Having the solution for the microfield, it is possible to transfer to the macroscopic field U. It is useful to rewrite (32) as

$$1 - \cos u = \frac{2a^2 \sinh^2 \zeta}{1 + a^2 \sinh^2 \zeta}.$$

By using this expression, in formula (9) the corresponding explicit expression for the macroscopic field of deformations can be obtained:

$$\rho(V_s^2 - V^2) U_{,q} = s \frac{2a^2 \sinh^2 \zeta}{1 + a^2 \sinh^2 \zeta} + \sigma.$$

Note that this even function of the argument $U_{,q} = f(\zeta)$ has a bell-like (soliton-like) form in spite of the fact that the initial microscopic field $u(\zeta)$ is, according to (32), a kinklike defect (with the center in q_0 and limits $u \to -\pi, \pi$ at the infinite distance from the center).

5. DEGENERACY OF SOLITARY WAVES INTO PERIODIC WAVES

The transition of the solitary waves (kinks and solitons) into the periodic localized waves is considered in more detail. Unlike periodic waves (regions 2–6 in Fig. 3), they belong to the first branch $G = -2\tilde{p}_1 = -2(\tilde{P} - \tilde{p}_2)$ (the inclined straight line in Fig. 3). It appears that the solitary waves of the second branch ($G = 0$) can transfer to the periodic ones as well. The transformation of kinks and solitons into the periodic localized waves occurs, as it was noted in previous sections, at definite stress. However, kinks and solitons of the first branch can degenerate into the periodic waves with decrease in stress (increase in the potential barrier $\tilde{p}_1$) as well. This is observed when stress overcomes the threshold determined from the relation $\tilde{p}_1 = \tilde{p}_2$ and the l_0^2/L^2 value becomes negative according to definition (29). At imaginary values of the width of the defect ($\lambda = -iL$) in the right-hand parts of solutions (28) and (33), the hyperbolic functions transform into trigonometric ones:

$$\begin{aligned} \cosh(q - q_0)/L &\to \cos(q - q_0)/\lambda, \\ \sinh(q - q_0)/L &\to -i\sin(q - q_0)/\lambda. \end{aligned} \quad (36)$$

As a result, solution (28) takes the form

$$\tan(u/2) = \alpha \cos(q - q_0)/\lambda. \quad (37)$$

However, here it is necessary to take into account the conditions at which the amplitude multiplier α, the same as the value u, should remain the real quantity ($\alpha^2 > 0$) at the inequality $l_0^2/L^2 < 0$. The analysis of the corresponding formula for α – (30) is given in previous sections. As can be seen from plots in Fig. 5, the conditions of the implementation of both inequalities ($\alpha^2 > 0$ and $l_0^2/L^2 < 0$) hold for a series of curves in the case of the periodic waves. They have different forms, depending on the velocity interval. In the case of solution (37), it is necessary to assume

$$1 + s^2/\lambda p \geq S \geq s^2/\lambda p \ (0 < V^2 < V_s^2);$$

$$S < 0 \ (V_s^2 < V^2 < V_k^2).$$

The results are given in Fig. 5. The condition $\alpha^2 > 0$ holds for the regions of curves lying above the abscissa axis and on the right to the boundary curve *5*. The condition $l_0^2/L^2 < 0$ is implemented by the branches lying to the left of the ordinate axis and above the abscissa axis (in the fourth quadrant). The amplitude depen-

dences, the upper regions of curves located between curves *5* and *7*, correspond to the subsonic branches corresponding to formula (37) (these are small regions coming to the right and upwards from the abscissa axis up to the ordinate axis). The supersonic branches of solution (37) begin on the ordinate axis and go to the left and upward with the output to the horizontal asymptote $V = V_k$, the boundary of the optical mode. The corresponding amplitude dependences are featured by the upper regions of the curves located to the right of curve *7*. They come under the abscissa axis ($\alpha^2 < 0$) implementing the transition to the other periodic solution.

This new periodic solution is obtained from relation (33) if the transition to the imaginary lengths L by means of the second relation in (36) is taken into account. In order to eliminate the imaginary multiplier in front of sine, the transition to the region of the amplitude dependences $\alpha^2 < 0$ is performed. They correspond to the region of curves in Fig. 5 lying below the abscissa axis. To keep the microdisplacement u in the region of real numbers, the amplitude multiplier of the form $a = i\alpha$ is taken. As a result, the periodic continuation of solution (32) is obtained:

$$\tan(u/2) = -a\sin(q - q_0)/\lambda. \qquad (38)$$

The mentioned curves under the abscissa axis directed to the side of infinitely high velocities but not coming below the level $\alpha^2 = -1$ are the periodic waves of the optical mode. In Fig. 5, they correspond to the branch in the field of imaginary values L coming upward and to the left. The branches corresponding to the intermediate ultrasonic range $V_s^2 < V^2 < V_k^2$ lie below the level of the optical oscillations. Their amplitudes are presented in Fig. 5 by the regions of curves also not coming below the level $\alpha^2 = -1$ but located between curves *5* and *7* ($1 < S < 0$).

Finally, the slow periodic waves corresponding to solution (38) are shown in Fig. 5 by the subsonic branches in the fourth quadrant as well. They start from the abscissa axis and conform to the originally stationary regular defects to which the amplitude dependences with infinitely decreasing (to the negative side) values, coming downward and to the left ($-\infty < \alpha^2 < -1$) correspond. The infinitely increasing amplitude multiplier in front of the sine in solution (38), the left-hand part of which is expressed in terms of the tangent of the sought function leads to the intensification, degeneracy of its smooth dependence on the argument. Figure 7 shows the plots of the microdisplacements $u(q/L)$ (38) for different values of the amplitude multiplier of the solution.

Obviously, the profile of the wave presenting a system of Π-like (localized) sequences or a regular sequence of sharp kinks with alternating signs reminding the plot of elliptical sine with the infinitely large period L in Fig. 7 corresponds to the high values of

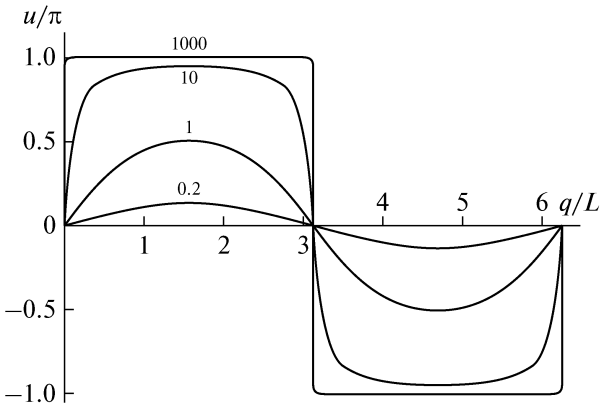

Fig. 7. Evolution of the form of the periodic solution depending on increase in the amplitude multiplier from 0.2 to 1000.

the amplitude multiplier (the microamplitude values $u \to -\pi, \pi$). In the limit the point of the transition of the phonon modes into the kinks ones is reached. At the beginning of the section, the criterion of this transition as a condition $\tilde{p}_1 = \tilde{p}_2$ was formulated. By opening it in accordance with formulas (11) and (12), the relation

$$\frac{2s^2 + \sigma}{\lambda p} = (1 - V_t^2/V_s^2) \qquad (39)$$

is obtained. Here, V_t is the wave velocity at the boundary of the phonon–kink transition. In this form the criterion of the transition gives a direct relation between stress and the transition velocity V_t.

The question about stability of the periodic waves arises at the transition of the solitary waves to the periodic ones. In this sense the result obtained by Wisem [13] is of interest. He has proven the necessary condition of the stability of the stationary periodic wave being the solution of the Klein–Gordon equation. At $\tilde{p}_2 = 0$ the studied Eq. (13) is its particular case. The necessary condition of Wisem is reduced to the requirement of increase in the intensity of the oscillations G with increase in the inverse period l_0/L. Since these values are related (for the waves of the first branch) by the relation $p(l_0/L)^2 = \tilde{p}_2 - G/2$, it is obvious that the condition of stability holds if $l_0^2/L^2 < 0$, i.e., in the case of periodic waves.

6. DISPERSION DEPENDENCES FOR LOCALIZED WAVES

The localized solutions of Eq. (13) have different dependences of the width of the wave localization L on parameters σ and V. Of most interest are the waves of the first type $G = -2\tilde{p}_1 = -2(\tilde{P} - \tilde{p}_2)$, to which

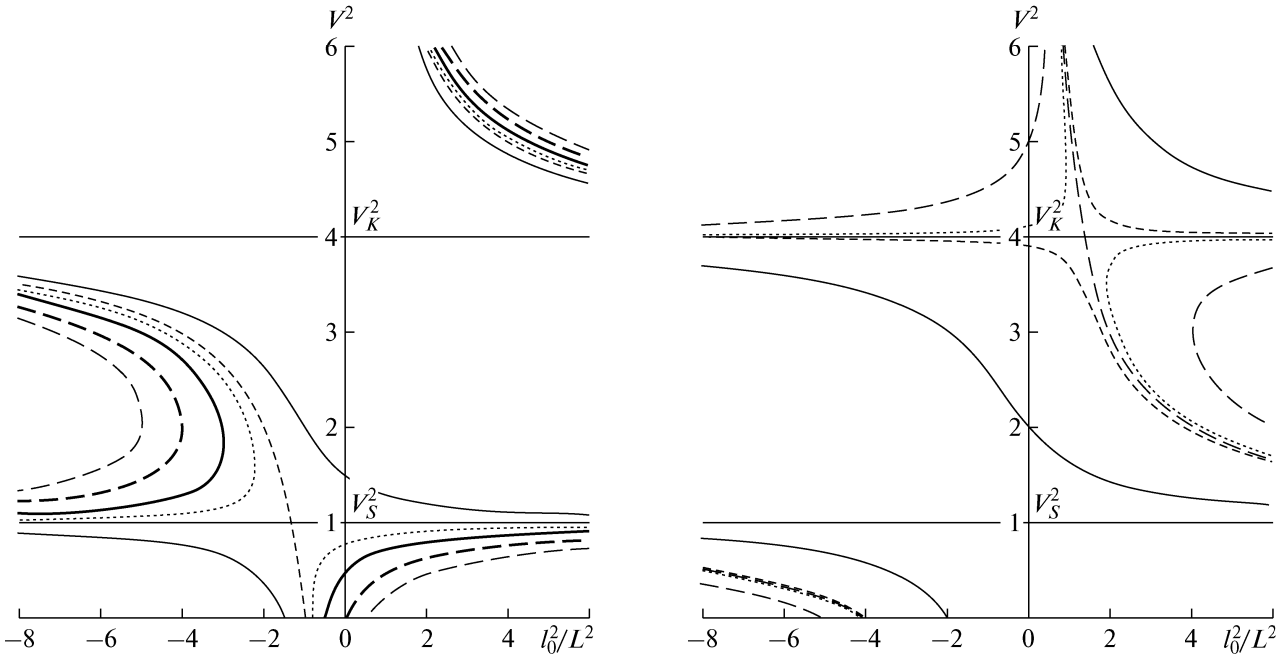

Fig. 8. Dependence of the velocity on the inverse width of the solitary wave ($l^2/L^2 > 0$) and on the inverse period.

dependence (29) corresponds. In the unfolded and transformed form it looks as:

$$\frac{l_0^2}{L^2} = \frac{S}{(1 - V^2/V_s^2)(1 - V^2/V_k^2)} - \frac{1}{(1 - V^2/V_k^2)}, \qquad (40)$$
$$l_0^2 = \frac{k}{p}, \quad S = \frac{s}{p}\varepsilon_m, \quad \varepsilon_m = \frac{(2s + \sigma)}{\lambda}.$$

Here, the "wave" multiplier $(1 - V^2/V_k^2)$ in the definition of the value $\tilde{l}_0^2$ (14) is transferred to the right-hand part of the formula.

The physical meaning of the parameter S attracts attention. It is simply proportional to the extreme value of the deformation $\varepsilon_m = \lambda U_{,x} = 2s + \sigma$ achieved in the region of the soliton or kink for the value $u = \pi$. At the positive value of the mechanical striction coefficient the parameter S the sign can change its sign depending on the value and sign of stress. On the other hand, S characterizes the relation between macro- and microstates.

Relation (40) is equivalent to the biquadratic equation with respect to V^2 having two roots $V_{\text{ac}}^2(L)$ and $V_{0p}^2(L)$ corresponding to the acoustic and optical branches. If the relationship is absent ($S = 0$, $\varepsilon_m = 0$), these roots are as follows:

$$V^2 = V_s^2, \qquad (41)$$

$$V^2/V_k^2 = 1 + L^2/l_0^2. \qquad (42)$$

The first relation is the result of the solution of the macroscopic wave equation (an arbitrary wave propagating at the velocity of the linear sound wave); the second relation determines the dependence of the velocity of the microdisplacement wave on the kink or soliton width. Both waves, according to the data, are independent, to each of them corresponding a branch in Fig. 8a. The first branch is a straight line parallel to the abscissa axis at the level of $V^2 = V_s^2$, the second branch (small dashes) crosses it and consists of the two regions of the hyperbole: supervelocity $V^2 \geq V_k^2$ (upper curve) and low-velocity $V^2 \leq V_k^2$ (lower curve). This is the so-called crossover (resonance) is degenerate if macro- and micromodes interact.

In the case of the tension macrodeformation ($S = \varepsilon_m = 0.5$ and $(s\sigma)/(\lambda p) = 0$), the crossover picture splits into two branches (two bold solid curves in Fig. 8a). Both branches represent one root of Eq. (40) having a breakup at $V^2 \leq V_k^2$. The supervelocity branch (bold curve $V^2 = V_s^2$) corresponds to the second root. The pair of the branches is drawn further apart the stronger the interaction (the larger the parameter S linearly dependent on stress). The values $S = \varepsilon_m = 1$ and $(s\sigma)/(\lambda p) = 0.5$ satisfy the curve denoted with bold dashes. For the pair of curves denoted with long thin dashes $S = \varepsilon_m = 1.5$ and $(s\sigma)/(\lambda p) = 1$. On the contrary, the curves closest to the crossover denoted by dots in Fig. 8a correspond to the negative values of the compression stress ($S = \varepsilon_m = 0.2$ and $(s\sigma)/(\lambda p) = -0.3$).

If the case of the negative parameter of the interaction $S = \varepsilon_m = -0.5$ and $(s\sigma)/(\lambda p) = -1$ (compression macrodeformations) is considered, it is seen that the crossover is allowed with the formation of other branches (solid thin curves in Fig. 8a). Now the waves of the intermediate range of the velocities appear in the region of real solutions of the localized waves ($l_0^2/L^2 > 0$) and low-velocity localized waves are not formed. They move to the imaginary region where the low-frequency periodic waves, which are supplied with the energy by the radio-frequency localized waves, can appear.

Note that in Fig. 8a the region of the negative values of the abscissa axis corresponds to the imaginary values of the defect width L. The corresponding regions of the branches do not present the real solutions to the solitary waves. However, they can make sense for the periodic solutions if the hyperbolic functions by means of which the localized waves are described transfer to the trigonometric ones according to the criterion (39). Then the positive interaction parameter is responsible for the energy transfer of the localized waves to the periodic waves. This case was considered in the previous section.

Note the following as well. The points of the abscissa axis in Fig. 8a by definition represent zero velocities, i.e., they are related to the static values of the width of the stationary defect for which

$$\frac{l_0^2}{L_0^2} = S - 1, \quad V = 0. \tag{43}$$

The bold dotted curve corresponding to the value $S = 1$ comes from the point $l_0^2/L^2 = 0$ on the abscissa axis. This means that the corresponding defect in the stationary state has the infinitely large width ($L_0 \to \infty$). If $S = 1.5$, then the corresponding curve (shown with long thin dashes) should come from the point $l_0^2/L_0^2 = 0.5$.

Relation (43) allows one to formulate the criterion of the coalescence of solitary stationary defects. Due to the fact that the left-hand part of expression (43) is positive, by opening the expression for S,

$$\frac{\lambda}{p}\varepsilon_m \geq 1 \to \sigma \geq \sigma_p, \quad \sigma_p = p\lambda/s - 2s.$$

The second inequality is rewritten with respect to stress. Here, the σ_p value is the threshold of the mobility of the defect. For dislocations it is known as the Peierls barrier [2]. Thence the coefficient of mechanical striction s can be calculated.

The defect width depends on stress: with increase in the positive (tension) stress the interaction parameter increases. Then, according to (43), the inverse defect width L increases as well, i.e., it is localized more strongly. In the limit the kink transforms into a percussion blast wave. Its width also depends on the velocity. This means that the form of the localized wave upon its propagation is not conserved: it is changed due to the exchange energy with the macroscopic mode.

Note two features of the change of the form of the localized wave. The first of them is concerned with the asymptotic freezing of this branch out at large values of the square of the inverse width, when the level of the velocity of the linear sound V_s is reached and the quasi-discontinuous wave appears. The second feature is revealed at the initial region of the sharp increase in the velocity (the width L is large), when the ordinate axis is crossed in the point $V_{ac} = 0$. The corresponding case is when the sufficiently smeared out kink or soliton, to which in this theory the solitary wave corresponds, can stop.

Dependence (42) of the velocity on the width of the solitary wave, "optical" branch $V_{0p}^2(L)$, which is the second root of Eq. (40), corresponds to the supersonic waves. In Fig. 8a it is shown with an upper curve. This curve, resembling a hyperbole, is asymptotically lowered to the limiting level, the typical velocity of the optical mode V_k. The value $L^{-1} \to \infty$, i.e., the width, for example, of the kink, becomes small, and the quasi-discontinuous wave is formed.

Dependences (41) and (42) have a presentation in the region of the imaginary values of the width L as well, when its square corresponds to negative values on the abscissa axis. In the figure this is the intermediate supersonic branch V_{a0} located in the interval of the velocity values $V_s^2 < V_{a0}^2 < V_k^2$. It has a simple physical meaning: it describes the periodic (nonlocalized) waves, which were considered in the previous section. It should be emphasized that these are special waves of switching of the interatomic bonds with the amplitude $u_m = \pi$, genetically related to the solitary waves by the general condition of the formation, when the constant G in Eq. (13) is given in a special way according to condition (21). Given the other choice of this constant the other periodic waves belonging to the regions 2–6 (Fig. 3) are possible.

The case of the strong compression stress at which the hardening parameter becomes a much negative quantity is of interest. If the corresponding hardening parameter becomes

$$S = \left(1 - \frac{V_k^2}{V_s^2}\right), \quad V_k^2 > V_s^2, \tag{44}$$

then the velocity of the optical mode $V = V_k$ is reached. This follows from relation (40), which takes the form

$$\frac{l_0^2}{L^2} = \frac{1 - V_k^2/V_s^2}{(1 - V^2/V_s^2)(1 - V^2/V_k^2)} - \frac{1}{(1 - V^2/V_k^2)}.$$

As can be seen from Fig. 8b, the corresponding branch crosses the level $V = V_k$ at the positive value of $l_0^2/L^2 > 0$, when the solitary waves propagate. The second crossing situation arises, which differs from the crossing situation considered in the beginning of this section (the resonance of acoustic and supersonic branches). In this case there is resonance of the supersonic and optical modes. This is typical for the tension stress, which weakens the lattice, leading to the appearance of standing defects.

The properties of the crystal undergo qualitative changes at large compression stress ($S \le 1 - V_k^2/V_s^2$). The crystal is strengthened, and it becomes rigid (diamond-like), losing plasticity. The relevant manifestation is that the defects, i.e., solitary waves (kinks and solitons) capable of stopping, do not appear in it. In this case there appear only the high-velocity branches of the traveling waves shown in Fig. 8b for $S = -1$ (solid thin curves), $S = -2.9$ (short thin dashes), $S = -3$ (bold dashes), $S = -3.1$ (points), and $S = -4$ (long thin dashes). The crossing situation is formed by the intersection of the curve $S = -3$ with horizontal line $V^2 = V_k^2 = 4$. In the first quadrant ($l_0^2/L^2 > 0$) the subsonic branches coming from the points of the abscissa axis $V = 0$ to which the stationary defects correspond are absent. The soliton and kink solutions are revealed in the supersonic range. Interestingly, there still exists the narrow region of the supersonic (optical) waves occupying the range of quite broad (weakly localized) formations:

$$0 < \frac{l_0^2}{L^2} \le \frac{V_k^2}{V_k^2 - V_s^2}.$$

Here, the equality sign is achieved at the value of the hardening parameter S presented by relation (44). This value is negative.

However, the branches of the low-velocity periodic waves coming from the negative region of the abscissa axis are located in the second quadrant ($l_0^2/L^2 < 0$) at the condition $S \le 1 - V_k^2/V_s^2$. At the zero velocities, these are stationary periodic superstructures with the period L/l_0. The traveling nonlinear waves exist only in super-velocity (optical) range.

7. TWO-DIMENSIONAL WAVES OF THE SINE-GORDON EQUATION IN INHOMOGENEOUS MEDIA

7.1. Main Equations of the Two-Dimensional Theory

Lagrangian variation (1) is the starting point, just as in the one-dimensional case. Now the invariant expression for the energy of macro- and microdeformations (taking into account their interactions: nonlinear mechanical striction, rearrangement of the microstructure under the action of macroscopic deformations) has the form

$$d = (1/2)[\lambda_{ijmn}U_{(i,j)}U_{(m,n)} + k_{ijmn}u_{(i,j)}u_{(m,n)} - (p - S_{ik}U_{(i,k)})(1 - \cos u_R)]; \quad u_R = \sqrt{u_x^2 + u_y^2}. \tag{45}$$

Here, U_i is acoustic displacements (the center of the inertia of pair of atoms in the unit cell); u_i are "optical" displacements (their mutual displacements); p is half of the energy of the activation of the rigid shift of sublattices; S_{ik} is the tensor of the striction coefficients; and λ_{ikmn}, k_{ikmn} are tensors of the coefficients of elasticity and microelasticity, respectively. The term with a multiplier $(1 - \cos u_R)$ presents the energy of the interaction of sublattices, which is chosen as a periodic function of microdisplacements. In this case (45) turns to be the invariant function with respect to mutual translations and rotation of sublattices. The variational equations of the motion of the macroscopic and microscopic modes have the form

$$\rho \ddot{U}_i = \sigma_{ij,j}, \tag{46}$$

$$\sigma_{ij} = \lambda_{ijmn}U_{(m,n)} - s_{ij}(1 - \cos u_R), \tag{47}$$

$$\mu \ddot{u}_i = k_{ijmn}u_{m,nj} + l_i P \sin u_R, \qquad P = p - s_{nj}U_{n,j}, \tag{48}$$

where ρ is the average density of the mass of atoms and μ is the reduced density of the pairs of atoms. The first equation is the equation of the elastic continuum, and the second equation takes into account the discrete structure of the lattice. The second term on the right in (48) corresponds to the interaction neighboring atom in the unit cell and takes into account the near order in the lattice. The quantity $l_i = u_i/u$ is the unit vector of the microdisplacement of the neighboring atom.

Equation (48) has the form of the generalized vector sine-Gordon equation with the variable coefficient P in front of sine since the coefficient includes the term of the macroscopic gradient of the displacement (macrodeformation). The latter, generally speaking, depends on coordinates and time according to Eq. (46). This circumstance is a quite interesting problem in physics of crystalline state. The issue is that the coefficient P is the effective interatomic potential barrier, the activation energy of the bonds. It is, as already noted, a quite sensitive instrument for controlling the microstructure and properties of the lattice by means of the macroscopic fields of deformations and stress. In the case of the one-dimensional field of the stress above, it was possible to consider stress and the coefficient P constant. This allowed finding a series of exact solutions of the sine-Gordon equation and analysis of the effect of the microstructure rearrangements on the propagation of the nonlinear waves. The generalized vector sine-Gordon equation in form (48) is too complicated for the analysis. It is possible to reveal a number of its exact solutions in the case when it is reduced

to a simpler form. This is achieved in the problems related to the deformations of thin plates, narrow gaps, and interphase regions.

The plane problem for the fields of macro- and microdisplacements is considered,

$$U_x = U_x(x, y, t); \quad U_y = U_y(x, y, t); \quad U_z = 0;$$
$$u_x = u_x(x, y, t); \quad u_y = u_y(x, y, t); \quad u_z = 0.$$

For a cubic crystal, the equations are

$$\rho \ddot{U}_x = \sigma_{xx,x} + \sigma_{xy,y}, \quad \rho \ddot{U}_y = \sigma_{yy,y} + \sigma_{yx,x}, \tag{49}$$

$$\mu \ddot{u}_x = -Pl_x \sin(u_x^2 + u_y^2)^{1/2} + K_1 u_{x,xx} + K_{23} u_{y,xy} + K_3 u_{x,yy}; \quad P = S(U_{x,x} + U_{y,y}), \tag{50}$$

$$\mu \ddot{u}_y = -Pl_y \sin(u_x^2 + u_y^2)^{1/2} + K_1 u_{y,yy} + K_{23} u_{x,yx} + K_4 u_{y,xx}; \quad S = S_{x,x} = S_{y,y}. \tag{51}$$

For the fields of stress in accordance with general formula (47),

$$\sigma_{xx} = \lambda_1 U_{x,x} + \lambda_2 U_{y,y} - S_{xx}(1 - \cos(u_x^2 + u_y^2)^{1/2}), \tag{52}$$

$$\sigma_{yy} = \lambda_2 U_{x,x} + \lambda_1 U_{y,y} - S_{yy}(1 - \cos(u_x^2 + u_y^2)^{1/2}), \tag{53}$$

$$\sigma_{yx} = \lambda_3 (U_{x,y} + U_{y,x}). \tag{54}$$

In the last expression the term with the coefficient S_{xy}, which is zero for the crystal of cubic symmetry, is omitted if the Cartesian coordinate system in the initial state is chosen so that its axes coincide with the crystallographic symmetry axes of the crystal. For crystals of other classes of symmetry, exclusive of triclinic and monoclinic syngonies, analogous gradient terms, but with less symmetrical coefficients, are obtained.

Additional simplifications are necessary for further analysis. Even in the two-dimensional case, (50) and (51) are a system of two coupled equations for the components of microdisplacements. This system can be reduced to the two separate equations of the sine-Gordon type only in particular cases, since it has the cross second derivatives of the $u_{y,xy}$, $u_{x,yx}$ type.

As shown in [13], in the extremely narrow nanoscale gap L wide, it is possible to restrict oneself to the consideration of near-surface high-gradient layers, which re exceedingly thin and spreading in the direction of the OY axis with the transverse displacements u_x that are small if compared with the longitudinal ones u_y. Therefore, the following restrictions are acceptable:

$$U_x \ll U_y, \quad \ddot{U}_x \ll \ddot{U}_y;$$
$$u_x \ll u_y, \quad \ddot{u}_x \ll \ddot{u}_y; \quad \partial u/\partial y \ll \partial u/\partial x. \tag{55}$$

Using these conditions, equations determining the two-dimensional fields of macro- and microdisplacements can be written in the zero approximation in small terms.

First the solution of macroscopic equations of motion (49) with key relations (52)–(54) is considered. After substitution of the latter in the former, they should be simplified by accepting conditions (55). By ignoring terms with derivatives $U_{x,yy}$, $(1 - \cos u_R)_y$ in the equation for its x-projection and terms of the form $U_{y,yy}$, $(1 - \cos u_R)_y$ in the equation for its y-projection, two second-order equations that are once integrated on the variable x are obtained. As a result, the first integrals are

$$\lambda_1 U_{x,x} + (\lambda_2 + \lambda_3) U_{y,y} - s_{xx}(1 - \cos u_R) = \sigma_0(y),$$
$$\lambda_3 U_{y,x} = \varepsilon_0, \quad u_R = \sqrt{u_x^2 + u_y^2}. \tag{56}$$

Here, $\sigma_0(y)$, $\varepsilon_0(y)$, $\varepsilon_{0,y}$ are the integration constants (the arbitrary function y) and derivative over this variable. The last relation (a very simple one due to the smallness of the layer thickness) is integrated, and the expression for the component U_y is obtained:

$$\lambda_3 U_y = \varepsilon_0(y).$$

By differentiating it over y, the derivative $U_{y,y}$ is found:

$$\lambda_3 U_{y,y} = x\varepsilon_{0,y}(y).$$

By combining this with (56), the expression for the sum of derivatives $(U_{x,x} + U_{y,y})$ is obtained. Then on the basis of the definition in (50),

$$P = p - S(U_{x,x} + U_{y,y}) = -\frac{S^2}{\lambda_1 - \rho V_1^2}(1 - \cos u) - \frac{S\sigma_0(y)}{\lambda_1 - \rho V_1^2} - \frac{S(\lambda_1 - \lambda_2 - \lambda_3 - \rho V_1^2)}{(\lambda_3 - \rho V_1^2)(\lambda_1 - \rho V_1^2)} x\varepsilon_{0,y} + p. \tag{57}$$

This formula is written in the final form with reference to dynamics when two waves of the macroscopic displacements propagating along the $0X$ and $0Y$ axes are considered. Here, V_1 and V_2 are their velocities.

Now Eqs. (50) and (51) for microdisplacements can be analyzed. The following simplifications are useful for their integration. Trigonometric terms with a small multiplier l_x in Eq. (50) are omitted and u is changed to u_y and l_y is changed to unity in Eq. (51). As a result, the system

$$\mu \ddot{u}_x \approx k_1 u_{x,xx} + k_{23} u_{y,xy}, \tag{58}$$

$$\mu \ddot{u}_y \approx k_1 u_{y,yy} + k_{23} u_{x,yx} + k_4 u_{y,xx} - P \sin u_y \tag{59}$$

is obtained. In the first equation, the term $u_{x,yy}$ is also omitted due to the smoothness of the field along the layer and the smallness of the microdisplacement component u_x in the transverse direction.

Let us move on to the dynamics of the stationary waves of microdisplacements. Ansatzes $x = x - v_1 t$, $y = y - v_2 t$, where v_1, v_2 are velocities of the waves of

microdisplacements propagating along axes $0X$ and $0Y$. Then Eq. (59) is rewritten as follows:

$$0 = K_1 u_{x,xx} + k_{23} u_{y,xy};$$
$$K_1 = k_1 - \mu v_1^2; \quad x = x - v_1 t; \quad y = y - v_2 t.$$

Then it is integrated once on x, which reduces it to a simple first-order equation. After its differentiation on y, with its help it is possible to exclude from (59) the cross derivative $u_{x,yx}$, which finally gives an equation of the sine-Gordon type

$$0 = K_4 u_{y,xx} + K_{23} u_{y,yy} - P\sin u_y;$$
$$K_4 = k_4 - \mu v_1^2; \quad K_{23} = k_1 - \mu v_2^2 + \frac{k_{23}^2}{\mu v_1^2 - k_1}. \tag{60}$$

It is important that, in front of the sine term, it has the coefficient P, which due to (57) turns out to be the function of coordinates. There are two equations for finding the fields $u_x(x, y)$, $u_y(x, y)$, which can be received in the analytical closed form.

The sine-Gordon equation, generally speaking, appears in many fields of modern natural science. It simulates the deformation of the nonlinear crystalline lattice [7–12], orientation structure of liquid crystals [14], orientation of spins in ferromagnets [15], metrics of surfaces [16], etc. It also appears during simulation of processes occurring in the terrestrial cortex [17], in molecular biology [18], in models of the field theory [19], and in physics of elementary particles [20].

Ar the present time, effective methods of solving the sine-Gordon equation are elaborated. However, the majority of methods are developed with reference to the case $P(x, y, t) = \text{const}$. This considerably limits the application of the sine-Gordon equation. In the mechanics of liquid crystals, the case $P(x, y, t) = \text{const}$ simulates the deformation of the long axes provided that the orientation continuum does not contain defects and the electromagnetic field is homogeneous. Otherwise $P(x, y, t) \neq \text{const}$. In differential geometry the sine-Gordon equation with $P(x, y, t) = \text{const}$ describes the metrics of the Chebyshev nets on the surface with constant curvature. If the curvature changes, then $P(x, y, t) \neq \text{const}$. In the mechanics of the nonlinear crystalline lattice, the case of the constant amplitude describes the deformation of the ideal lattice by the field of homogeneous stress. The deformation of the real lattice with the structure defects (dislocations, disclinations, nuclei of pores, cracks, etc.) by the field of inhomogeneous stress (deformations) is also described by sine-Gordon equation (48) with a variable amplitude in form (60) alongside Eq. (46).

7.2. Functionally Invariant Solutions of the Sine-Gordon Equation with the Variable Amplitude

When carrying out analysis of sine-Gordon equation (60) with a variable amplitude, it is reasonable to rewrite it in a more suitable reduced form:

$$\frac{\partial^2 u_y}{\partial \chi^2} + \frac{\partial^2 u_y}{\partial \xi^2} - \frac{1}{v^2}\frac{\partial^2 u_y}{\partial \tau^2} = P(\chi, \xi, \tau)\sin u_y;$$
$$x = \chi\sqrt{K_4}, \quad y = \xi\sqrt{K_5}, \quad t = \tau v\sqrt{\mu}. \tag{61}$$

The solution of Eq. (61) is searched for in the form

$$\tan u_y/4 = e^{\varphi(\chi, \xi, \tau)}. \tag{62}$$

By substituting (62) in (61), we make sure that Eq. (61) is solved if the function $\varphi(\chi, \xi, \tau)$ satisfies simultaneously two equations, the homogeneous wave equation,

$$\frac{\partial^2 \varphi}{\partial \chi^2} + \frac{\partial^2 \varphi}{\partial \xi^2} - \frac{1}{v^2}\frac{\partial^2 \varphi}{\partial \tau^2} = 0, \tag{63}$$

and the eikonal equation,

$$\left(\frac{\partial \varphi}{\partial \chi}\right)^2 + \left(\frac{\partial \varphi}{\partial \xi}\right)^2 - \frac{1}{v^2}\left(\frac{\partial \varphi}{\partial \tau}\right)^2 = P(\chi, \xi, \tau). \tag{64}$$

The latter is the basic equation in geometric optics [20]. It describes the propagation of the wave surface (surfaces of the same phase) in medium with the inhomogeneous refraction coefficient of depending also on time. Equation (64) is studied in many papers [19–25]. The solution of Eq. (61) is also

$$\tan u_y/2 = e^{\varphi(\chi, \xi, \tau)},$$

provided that $\varphi(\chi, \xi, \tau)$ satisfies simultaneously two equations,

$$\frac{\partial^2 \varphi}{\partial \chi^2} + \frac{\partial^2 \varphi}{\partial \xi^2} - \frac{1}{v^2}\frac{\partial^2 \varphi}{\partial \tau^2} = P(\chi, \xi, \tau), \tag{65}$$

$$\left(\frac{\partial \varphi}{\partial \chi}\right)^2 + \left(\frac{\partial \varphi}{\partial \xi}\right)^2 - \frac{1}{v^2}\left(\frac{\partial \varphi}{\partial \tau}\right)^2 = 0. \tag{66}$$

Thus, integration of the sine-Gordon equation with the variable amplitude was reduced to finding the function $\varphi(\chi, \xi, \tau)$ which is simultaneously a solution of Eqs. (63), (64) or (65), (66). The most perspective approach to finding such a function is a method of the construction of the functionally invariant solutions of the differential equations.

The first way. The solution of Eq. (63) is present as

$$\varphi = F(\alpha).$$

Here, $F(\alpha)$ is an arbitrary function and the argument $\alpha(\chi, \xi, \tau)$ is the root of the equation linear on variables (χ, ξ, τ):

$$\chi l(\alpha) + \xi m(\alpha) - v^2 \tau q(\alpha) + g(\alpha) = 0 \tag{67}$$

and the coefficients $l(\alpha)$, $m(\alpha)$, $q(\alpha)$, and $g(\alpha)$ are arbitrary functions related by one condition,

$$l^2(\alpha) + m^2(\alpha) = v^2 q^2(\alpha). \tag{68}$$

Taking into account (68), the solution of wave equation (63) is

$$\varphi = F(\alpha), \quad \alpha = \tau - \theta\chi \pm \xi\sqrt{\frac{1}{v^2} - \theta^2}, \quad \theta = \text{const}. \tag{69}$$

If $\theta^2 < 1/v^2$, the Ansatz is real and the solution of (69) is a planar wave. With the plus sign, the wave goes to the boundary of the semispace $y = 0$, and with the minus sign, the wave goes from the boundary $y = 0$. The real Ansatz allows one to build [19] functionally invariant solutions of the sine-Gordon equation with the constant amplitude ($P = 1$). If $\theta^2 > 1/v^2$, the real Ansatzes transfer to the complex-conjugate ones

$$\zeta = \tau - \theta\chi - i\xi\sqrt{\frac{1}{v^2} - \theta^2}, \quad \tilde{\zeta} = \tau - \theta\chi - i\xi\sqrt{\frac{1}{v^2} - \theta^2}.$$

Since the solution of the sine-Gordon equation is expected to be real, then the function

$$\tan u_y/4 = e^{\varphi(\chi,\xi,\tau)}, \quad \varphi(\chi,\xi,\tau) = \frac{1}{2}[F(\zeta) + F(\tilde{\zeta})] \tag{70}$$

is solution (61) with the amplitude

$$P(\chi,\xi,\tau) = \left(\theta^2 - \frac{1}{v^2}\right)F'(\zeta)F'(\tilde{\zeta}). \tag{71}$$

Here and below the stroke means the derivative on the argument. Since $F(\zeta)$ is an arbitrary function, (71) presents a wide class of amplitudes $P(\chi, \xi, \tau)$ for which (70) there is the solution of the sine-Gordon equation.

Figure 9 shows the spatial distribution of the effective barrier $P(x, y, t)$ with a singularity in the point (a) and the corresponding localized perturbation of the field u_y of the microdisplacements of atoms, which in a nonperturbed state had the form of the kink (b). Ansatz α can be chosen in another way. For the sake of simplicity, assume that

$$vq(\alpha) = 1, \quad g(\alpha) = 0.$$

Then the condition (68) holds if

$$l = \cos\alpha, \quad m = \sin\alpha. \tag{72}$$

By substituting (72) in (67), find

$$\chi\cos(\alpha) + \xi\sin\alpha = v\tau,$$

$$\alpha = \varphi \pm \arccos\frac{v\tau}{r} + 2n\pi, \quad \tan\varphi = \frac{\xi}{\chi},$$

$$r = \sqrt{\chi^2 + \xi^2}, \quad n = 1, 2\ldots .$$

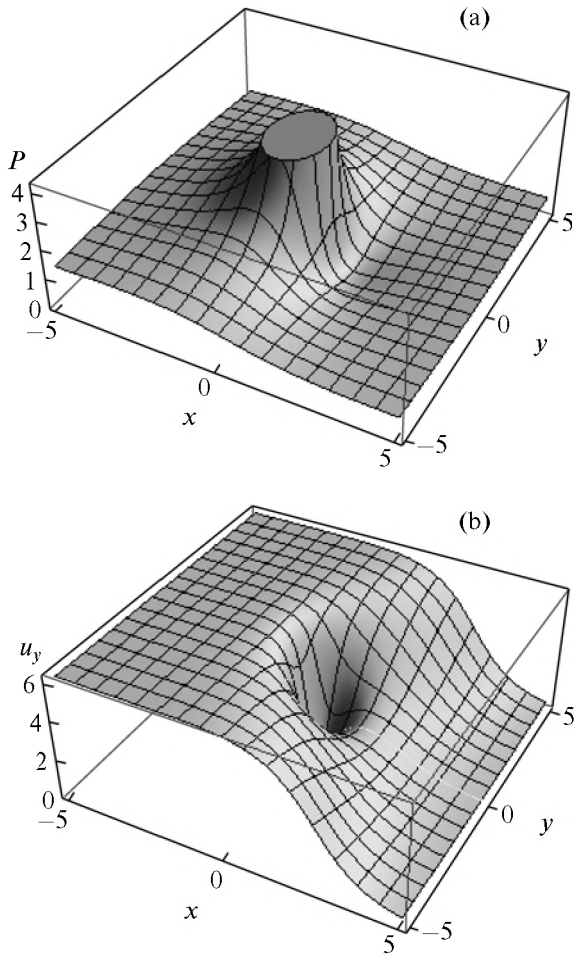

Fig. 9. Spatial distribution the effective barrier $P(x, y, t)$ with the singularity in the point (a); the corresponding localized perturbation of the field u_y of the microdisplacements of atoms which in the non-perturbed state had the form of the kink (b).

The direct calculation shows that

$$\varphi = A(\alpha) + \frac{B(\alpha)}{s}, \quad s^2 = \chi^2 + \xi^2 - v^2\tau^2 \tag{73}$$

satisfies wave equation (63). Here, $A(\alpha)$, $B(\alpha)$ are arbitrary functions. Equation (64) holds if

$$P(\chi,\xi,\tau) = \frac{B^2(\alpha)s^4.}{s^4} \tag{74}$$

Thus, (73) is a solution of the sine-Gordon equation with the amplitude (74). Note that in this case solution (73) and amplitude (74) turn out to be singular. At the initial moment of time ($\tau = 0$), the singularity is found in the point ($\chi = 0$, $\xi = 0$), and in the following time moments it transforms in a circumference with the radius $v\tau$.

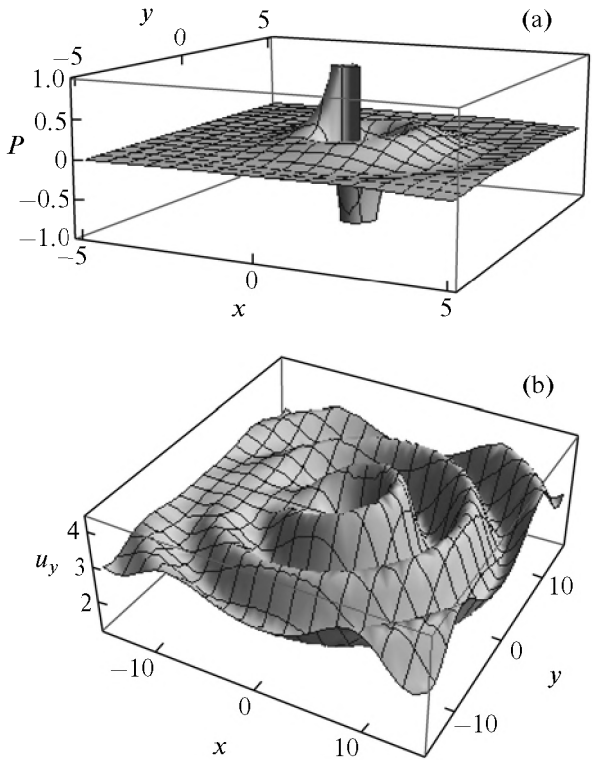

Fig. 10. Spatial distribution the effective barrier $P(x, y, t)$ with the singularity in the point (a); the corresponding localized perturbation of the field u_y of the microdisplacements of atoms (b). The singularity spreads from the center in the form of the concentric circles.

Here is the second way. The Ansatz $\alpha(\chi, \xi, \tau)$ is determined from the equation

$$[\chi - \zeta(\alpha)]^2 + [\xi - \eta(\alpha)]^2 = v^2(\tau - \alpha)[x - \xi(\alpha)]^2 + [y - \eta(\alpha)]^2 = v^2(t - \alpha), \quad (75)$$

and the function

$$\varphi(\chi, \xi, \tau) = \frac{f(\alpha)}{\sqrt{n}}$$

is constructed. Here,

$$n = l(\alpha)(\chi - \zeta) + m(\alpha)(\xi - \eta) - v^2 q(\alpha)(\tau - \alpha)$$

and $l(\alpha)$, $m(\alpha)$, $q(\alpha)$, $\zeta(\alpha)$, $\eta(\alpha)$ and $g(\alpha)$ are arbitrary functions related by the two relations

$$l(\alpha)\zeta'(\alpha) + m(\alpha)\eta'(\alpha) = v^2 q(\alpha),$$
$$l^2(\alpha) + m^2(\alpha) = v^2 q^2(\alpha).$$

The function $\varphi(\chi, \xi, \tau)$ satisfies wave equation (63) and eikonal equation (64) with the amplitude

$$P(\chi, \xi, \tau) = \frac{f^2(\alpha)}{2n^2}\frac{w}{\sigma} - \frac{ff'}{n\sigma},$$

$$P(x, y, t) = \frac{f^2(\alpha)}{2\tau^2}\frac{w}{\sigma} - \frac{ff'}{\tau\sigma},$$

$$w = l'(\alpha)(\chi - \zeta(\alpha)) + m'(\alpha)(\xi - \eta(\alpha)) - v^2 q'(\alpha)(\tau - \alpha), \quad (76)$$

$$\sigma = \zeta'(\alpha)(\chi - \zeta(\alpha)) + \eta'(\alpha)(\xi - \eta(\alpha)) - v^2(\tau - \alpha).$$

Consequently, $\tan u_y/4 = e^{\varphi(\chi, \xi, \tau)}$ is the solution of the sine-Gordon equation with amplitude $P(\chi, \xi, \tau)$-determined relation (76). Note the simple particular cases of the found solution. Let

$$vq(\alpha) = 1, \quad l = \cos\beta, \quad m = \sin\beta,$$
$$\zeta = v\alpha l, \quad \eta = v\alpha m, \quad \beta = \text{const}.$$

Then

$$n = x\cos\beta + y\sin\beta - v\tau, \quad \sigma = vn, \quad w = 0, \quad (77)$$

$$\alpha = \frac{s^2}{2\sigma}, \quad P(\chi, \xi, \tau) = -\frac{f(\alpha)f'(\alpha)}{\sigma}. \quad (78)$$

It is seen from (77) and (78) that, in this case, the amplitude $P(x, y, t)$ has a singularity on a line which spreads parallel to itself with the velocity v. If $\theta = 0$, the line degenerates into a singular point, which moves on the χ axis with the velocity v. If $\theta = \pi/2$, the singular point moves on the ξ axis. The second particular case is implemented if

$$\zeta(\alpha) = 0, \quad \eta(\alpha) = 0, \quad l(\alpha) = 1,$$
$$m(\alpha) = i, \quad q(\alpha) = 0.$$

Then

$$n = \chi + i\xi, \quad \alpha = \tau - \frac{r}{v}, \quad w = 0, \quad \sigma = -vr$$

and φ is the Poisson wave function

$$\varphi = \frac{f(\alpha)}{\sqrt{\chi + i\xi}}.$$

The real wave functions are

$$\varphi_+(\chi, \xi, \tau) = \frac{f(\alpha)}{r}\sqrt{r + \chi},$$

$$\varphi_-(\chi, \xi, \tau) = \frac{f(\alpha)}{r}\sqrt{r - \chi}.$$

The functions (φ_+, φ_-) are the solutions of Eq. (64) if

$$P_+(\chi, \xi, \tau) = \frac{f^2}{2r^3} + \frac{ff'(r + \chi)}{nr^3},$$

$$P_-(\chi, \xi, \tau) = \frac{f^2}{2r^3} + \frac{ff'(r - \chi)}{nr^3}.$$

Figure 10 shows the spatial distribution of the effective barrier $P(x, y, t)$ with the singularity in the point (a)

and the corresponding perturbation of the field u_y of the microdisplacements of atoms (b). The singularity spreads from the center in the form of concentric circles.

The found solutions of the sine-Gordon equations with the variable amplitude are built on basis of the function $\varphi(\chi, \xi, \tau)$ satisfying Eqs. (63) and (64). In a similar manner Eq. (61) can be solved on the basis of the function $\varphi(\chi, \xi, \tau)$, which satisfies Eqs. (65) and (66). An example of such an approach is given below.

The Ansatz $\alpha(\chi, \xi, \tau)$ is once again chosen as the root of Eq. (75). It is easy to show that an arbitrary function $f(\alpha)$ of the Ansatz $\alpha(\chi, \xi, \tau)$ satisfies Eq. (66). Equation (65) is solved if

$$P(\chi, \xi, \tau) = \frac{f'(\alpha)}{\sigma}. \quad (79)$$

The σ value is determined by relation (65). Thus,

$$\tan u_y/2 = e^{f(\alpha)} \quad (80)$$

is the solution of Eq. (84) if $\alpha(x, y, t)$ is the root of (75) and the amplitude $P(\chi, \xi, \tau)$ is (79).

The spatial distribution of the effective barrier $P(x, y, t)$ with the singularity on the line (a) and the corresponding perturbation of the field u_y of the microdisplacements of atoms (b) is given in Fig. 11. This simple example is used to show how the choice of the arbitrary function $f(\alpha)$ can be elaborated. Let expressions (57) and (79) be identical for the effective barrier P determined by the given choice and the problem about the deformation of a thin layer. To this end, in formula (57) it is necessary to express the term $(1 - \cos u_y)$ first in terms of $\tan u_y/2$ and then in terms of the function $f(\alpha)$ according to (80)

$$1 - \cos u_y = \frac{2\tan^2 u_y/2}{1 + \tan^2 u_y/2} = 2\frac{e^{f(\alpha)}}{e^{f(\alpha)} + e^{-f(\alpha)}}.$$

By using this expression in (57) and equalizing it to the right-hand part of definition (79), the condition of the consistency of the expressions for the potential barrier,

$$\frac{f'(\alpha)}{\sigma} = -\frac{2S^2}{\lambda_1 - \rho V_1^2}\frac{e^{f(\alpha)}}{e^{f(\alpha)} + e^{-f(\alpha)}}$$
$$-\frac{S\sigma_0(y)}{\lambda_1 - \rho V_1^2} - \frac{S(\lambda_1 - \lambda_2 - \lambda_3 - \rho V_1^2)}{(\lambda_3 - \rho V_1^2)(\lambda_1 - \rho V_1^2)}x\varepsilon_{0,y} + p$$

is found. It may be considered as the equation for additional definition of the arbitrary function $f(\alpha)$. It, just as Eq. (57), applies to dynamics,

$$\mu\ddot{u}_y \approx K_5 u_{y,yy} + K_4 u_{y,xx} - P\sin u_y;\ K_5 = K_1 + K_{23}^2/K_1.$$

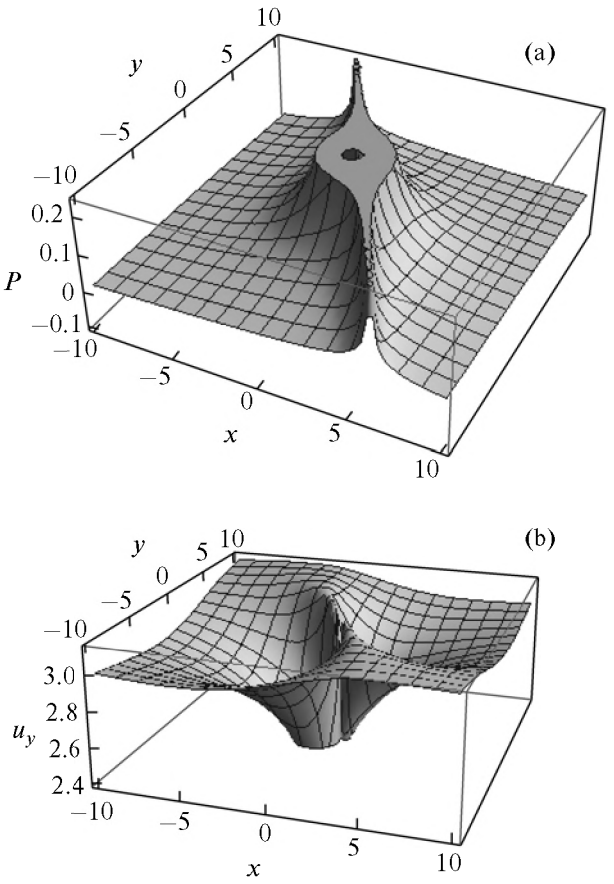

Fig. 11. Spatial distribution the effective barrier $P(x, y, t)$ with the singularity on the line (a); the corresponding localized perturbation of the field u_y of the microdisplacements of atoms (b).

8. CONCLUSIONS

On the basis of the discrete-continuum model of the complex lattice proposed earlier, a theory of nonlinear waves in solid state that allows one to take into account in the long-wave approximation the cardinal changes of the lattice structure at deformation (mechanical striction) is developed. The structural changes are described by the field of the microdisplacements of the neighboring atoms in the unit cell. In addition, the conventional macroscopic displacements taking into account the motion of the cells themselves are introduced. The dynamic equations in the linearized classical variant are reduced to the known equations of the propagation of the acoustic and "optical" modes established already in the works of Carman, Born, and Huang Kun. The variational approach proposed for the first time by E. and F. Cosserat (10 years before F. Klein and E. Neter) is generalized here to the translational internal degrees of freedom of the crystalline lattice.

The obtained nonlinear equations are related by the micromechanism of mechanical striction. As a result, the effect of the change of the interatomic

potential barriers at the impact of the external stress is described, the appearance of the structure defects in the field of the critical stress, and their motion as localized waves, as well as relaxation, are predicted.

In the developed nonlinear theory, the localized waves of the kink and soliton type describing the propagation and relaxation of the defects of packing and dislocations, as well as their transition in the nonlinear periodic waves at the strong compression, are considered. They turn out to be solutions of the nonlinear sine-Gordon equation.

In the one-dimensional case, this equation has constant coefficients. The mechanism of mechanical striction depending on stress and striction coefficients is implemented in the phenomena of hardening (making brittle) and weakening (plastification) of the crystal. The appearance of slow subsonic, fast supersonic, and superfast waves of the optical mode is related with these phenomena. The mutual effect of the acoustic and optical modes (macroscopic and microscopic fields) leads to the nuclei of defects being the functions of the macroscopic stress and velocities of the modes. Moreover, both macroscopic and microscopic localized wave packages describing the distortions of the macroscopic continuum and distortion of the microstructure appear.

The determinative parameter of the dynamic phenomena is the effective potential interatomic barrier dependent on stress and propagation velocities. It has three values (three bifurcation points) that determine the limits of stability of the lattice experiencing in statics cardinal rearrangement depending on the value and sign of the external stress. In dynamics the dependence of the potential barrier on the propagation velocity of the localized wave appears in addition. In particular, at a definite velocity, the periodic wave transfers to the localized one and vice versa. This process of the rearrangement is characterized by the threshold values of stress. The conditions of the formation of the quasi discontinuous waves are revealed.

The planar problems that require the analysis of the (2+1) sine-Gordon equations with the variable coefficients in front of the sine term are considered. This term is an effective interatomic potential barrier dependent on the external stress (macroscopic deformations), which, as a rule, are functions of coordinates and even time. The methods of building the solutions corresponding to the generalized sine-Gordon equation are elaborated. A series of its solutions describing the interaction of the localized nonlinear wave with the inhomogeneous perturbation of the above coefficient due to the structural changes of the crystal in the field of the external inhomogeneous stress is built. The methods of building similar solutions were proposed earlier [26].

ACKNOWLEDGMENTS

The study was performed in the framework of the fundamental investigation of the Presidium of the Russian Academy of Sciences with partial support of the Russian Foundation for Basic Research, projects nos. 07-01-00213 and 09-08-00634.

REFERENCES

1. M. Born and Kun Huang, *Dynamical Theory of Crystal Lattices* (Clarendon, Oxford, 1985; Inostr. Liter., Moscow, 1958).
2. A. M. Kosevich, *Theory of Crystal Lattice. Physical Mechanics of Crystals* (Vishcha shkola, Kharkov, 1988) [in Russian].
3. I. A. Kunin, *Theory of Elastic Media with Microstructure* (Nauka, Moscow, 1975) [in Russian].
4. E. Cosserat, *Theorie des corps deformables* (Lib. Sci. Hermann et Fils, Paris, 1909) [in French].
5. V. I. Erofeev and V. M. Rodyushkin, Akust. Zh. **38**, 1116 (1992) [Sov. Phys. Acoust. **38**, 611 (1992)].
6. A. I. Potapov and V. M. Rodyushkin, Akust. Zh. **47**, 407 (2001) [Acoust. Phys. **47**, 347 (2001)].
7. S. A. Lisina, A. I. Potapov, and V. F. Nesterenko, Akust. Zh. **47**, 685 (2001) [Acoust. Phys. **47**, 598 (2001)].
8. O. V. Rudenko, A. I. Korobov, and M. Yu. Izosimova, Akust. Zh. **55**, 172 (2009) [Acoust. Phys. **55**, 153 (2009)].
9. E. L. Aero, J. Eng. Mathem. **55**, 81 (2006).
10. E. L. Aero and A. N. Bulygin, Izv. Ross. Akad. Nauk: Mekh. Tverd. Tela, No. 5, 170 (2007).
11. E. L. Aero and A. N. Bulygin, Vych. Mekh. Sploshn. Sred **1** (1), 14 (2008).
12. A. V. Porubov, E. L. Aero, and G. A. Maugin, Phys. Rev. E **79**, 046608 (2009).
13. G. Whitham, *Linear and Nonlinear Waves* (Wiley, New York, 1974; Mir, Moscow, 1977).
14. P. G. De Gennes, *The Physics of Liquid Crystals* (Claredon, Oxford, 1974).
15. P. Guéret, IEEE Trans. Magnet., 751 (1975).
16. P. L. Chebyshev, Usp. Mat. Nauk **1** (2), 38 (1946).
17. V. G. Bykov, *Nonlinear Wave Processes in Geological Media* (Dal'nauka, Vladivostok, 2000) [in Russian].
18. A. S. Davydov, *Solitons in Bioenergetics* (Naukova Dumka, Kiev, 1986) [in Russian].
19. L. A. Takhtadzhyan and L. D. Faddeev, Teor. Mat. Fiz. **21**, 160 (1974).
20. M. Born and E. Wolf, *Principles of Optics* (Pergamon, New York, 1968).
21. J. Frenkel and T. Kontorova, J. Phys. Acad. Sci. USSR, 137 (1939).
22. R. M. Miura, *Backlund Transformations, the Inverse Scattering Method, Solitons, and Their Applications,* Lecture Notes Math. vol. 515 (Springer, Berlin, 1976).
23. R. Hirota, J. Phys. Soc. Jpn., 1459 (1972).
24. S. L. Sobolev, Tr. Matem. Inst. Steklova **5**, 259 (1934).
25. H. Bateman, *The Mathematical Analysis of Electrical and Optical Wave-Motion: On the Basis of Maxwell's Equations* (Dover, New York, 1955).
26. E. L. Aero, A. N. Bulygin, and Yu. V. Pavlov, Teor. Mat. Fiz. **158**, 370 (2009) [Theor. Math. Phys. **158**, 313 (2009)].